Journal of Ceramic Processing Research. Vol. 18, No. 12, pp. 843~847 (2017)

J O U R N A L O F
Ceramic Processing Research

Crystal structure and microstructure of metal carbides in Ni superalloy prepared by investment casting

Jong Bum Park[a,b], Jung-Il Lee[b], Kyung-Hwan Jung[c], Kang Min Kim[c,]* and Jeong Ho Ryu[b,]*

[a]*Chunji Corporation, Eunbong-ri 233-1, Yeoju, Gyeonggi 12663, Korea*

[b]*Department of Materials Science and Engineering, Korea National University of Transportation, Chungju, Chungbuk 27469, Korea*

[c]*Korea Institute of Industrial Technology, Gangneung, Gangwon 25440, Korea*

Rene 80, as a representative Ni-based superalloy for producing jet turbine blades, shows superior mechanical properties and microstructure stability during high-temperature engine operation. This study attempts to provide a deep insight into the microstructure of as-cast Rene 80 prepared by the investment casting method. For better understanding of the microstructure, the characterization of the samples was performed using optical microscopy (OM), field emission scanning electron microscopy (FE-SEM), and energy dispersive spectroscopy (EDS) techniques. Microstructural investigation shows that the as-cast microstructure of this alloy consists of a dendritic γ matrix, an interdendritic γ/γ' phase, a γ' phase, and MC and $M_{23}C_6$ carbides. Because of its high chromium content, the dominant phase was the $M_{23}C_6$-type carbide, whereas other elements in the alloy lead to the MC-type carbide. In this study, the as-cast microstructure was a γ/γ' dendritic matrix, with precipitation of a secondary phase, such as the $M_{23}C_6$ carbides, at the grain boundaries and interdendritic zones.

Key words: Ni superalloy, Rene 80, Investment casting, Microstructure, Metal carbide.

Introduction

Nickel-based superalloys are important materials for aerospace and power plant applications where high-temperature strength and creep resistance are critical [1]. The cast nickel-based superalloy Rene 80 is commonly used to manufacture the first- and second-stage turbine blades in modern jet engines owing to its excellent combination of high stress-rupture strength with thermal fatigue and hot corrosion resistance [2-4]. Rene 80 is generally used at a temperature of 760-982 °C and the microstructure of Rene 80 consists of the γ matrix, γ' phase precipitates in the γ matrix, and metal carbides. The γ' phase, which precipitates during heat treatment, is derived from the ordered face-centered cubic (FCC) crystal structure ($L1_2$), with corners of the unit cell occupied by Al or Ti atoms and face centers occupied by Ni atoms [5].

The most significant contributor to the strength of a nickel-based superalloy is the coherent precipitate of the γ' phase [6, 7]. To a large extent, the high-temperature strength and microstructural stability of a nickel-based superalloy rely on the formation of the γ' phase and its volume fraction, size and distribution [8]. An increase in the γ' volume fraction enhances the γ' solvus temperature, which enables the alloy to retain strength at high service temperature [9]. The presence of up to 70% of the ordered γ' phase provides significant strength to nickel-based superalloys [10].

Metal carbides also play a complex role in nickel-based superalloys, whose high-temperature properties can be improved in many circumstance if the proper proportion of carbon is present [11]. The coarse primary carbide of type MC is rich in Ti, Mo and W elements, M_6C carbide is rich in Ni, Co, Mo and Cr elements, and $M_{23}C_6$ carbide is rich in Cr element at the grain boundaries [12]. Metal carbides are prone to precipitate at the grain boundaries, which has a beneficial effect on the high-temperature strength via the inhibition of grain boundary sliding. However, the precipitate of metal carbides can sometimes facilitate crack initiation and propagation, and the function of metal carbides in nickel-based superalloys mainly depends on their geometry and distribution [13].

The script-like and elongated metal carbides can precipitate when the carbon content in the superalloy is too high impairing its mechanical properties. Moreover, the script-like and elongated carbides may also cause change the fracture modes of the superalloy from the typical intergranular mode to transgranular and intergranular mixed modes [14]. This work aimed to provide additional information on the microstructure of the metal carbide phases in the Rene 80 Ni superalloy prepared by investment casting, and to evaluate their possible transformation during solidification and cooling in an industrial environment.

*Corresponding author:
Tel : +82-43-841-5384, 82-33-649-4025
Fax: +82-43-841-5380, 82-33-649-4010
E-mail: jhryu@ut.ac.kr, kmkim@kitech.re.kr

Experimental

The chemical compositions of the cast nickel-based superalloy Rene 80 is Ni-14.60Cr-3.97W-4.50Mo-8.69Co-3.01Al-4.94Ti-0.17C (wt.%). The alloy was melted in an induction furnace under an Ar atmosphere. In the first step, the raw materials and mold were prepared. A mold was prepared using meltable materials, which are mainly used in the production of low-weight casting with a very smooth surface. A model made of a material with a low melting point, such as a type of wax (paraffin, stearin), was gradually covered by layers of mixtures, each with different granulometry, until the mold was obtained, i.e., a shell with 5-7 mm thick walls. When the model melts, it leaves a cavity that corresponds strictly to the shape of the desired model, and the shell can be used as a precise casting mold. Prior degassing is required for nickel, chromium and cobalt. They were annealed at 1000-1100 ºC, at pressures of 0.18-0.23 mbar. These metals were gradually charged into the highly luminous corundum crucible of an induction vacuum furnace.

Melting and casting may be performed under vacuum or in an argon atmosphere. If argon is used, it must be of extremely high purity (99.99%), and the pressure in the furnace receptor should be maintained below 0.10 Mbar. The mold was preheated to a temperature of 950-1030 ºC. The casting temperature was 1490-1530 ºC. The shell mold material and wall thickness enabled cooling control, along with grain size and shape control, which can influence the mechanical characteristics. By monitoring the pressure change, the beginning and end of the secondary degassing can be observed. Owing to the precise vacuum casting process characteristics, the obtained samples have accurate dimensions and good surfaces, without the need for additional sandblasting.

The bulk chemical composition was measured via wavelength dispersive X-ray fluorescence (WD-XRF, Rigaku, ZSX Primus II). The phase of the as-cast sample was identified using X-ray diffractometry (XRD, Bruker ASX, D8 Advance, Germany), and the XRD patterns were obtained using Cu Kα radiation. The preparation of samples for optical microscopy (OM) and field emission scanning electron microscopy (FE-SEM) was carried out using conventional procedures for grinding using SiC abrasive papers, from No. 200 up to No. 2000, and polishing using 1.0 μm diamond abrasive. Next, the specimens were thoroughly cleaned to remove any polishing residue. Then, the surface of the sample was etched for about 40 s in a solution of 50 ml HCl, 25 ml HNO_3, and 2 g $CuCl_2$ in 200 ml H_2O [15]. OM, with magnification from 100 × to 400 ×, was used to obtain a wide field of view. The high magnification was used to identify different phases. The samples were examined by field emission scanning electron microscopy (FE-SEM) using a JEOL JSM-7610F microscope, and the energy-dispersive spectroscopy (EDS) techniques was also employed to provide a more accurate characterization of the different precipitated phases, even though the EDS technique provides a semi-quantitative analysis. The system used was EDAX (Oxford X-max) equipped with an LN2 free silicon drift detector.

Results and Discussion

Fig. 1(a) shows the crystal structure of the as-cast Ni-base Rene 80 superalloy sample analyzed using XRD in the scan range of 20-80 º. The as-cast sample exhibited the prominent diffraction lines of the γ and γ' phases with MC and $M_{23}C_6$ metal carbides. Inspection of the XRD pattern revealed that the three peaks in the as-cast sample could be attributed to the (111), (200), and (220) planes of an FCC phase (γ matrix). The (010), (111), (200) and (220) planes of the γ' phase with FCC structure were observed, and the dominant precipitations of the metal carbides were MC and $M_{23}C_6$ [16]. Fig. 1(b) shows the optical micrograph of the as-cast sample. The microstructure of the as-cast Rene 80 consists of a two-phase γ/γ' microstructure with a dendrite segregation pattern. The average spacing of the primary and secondary dendrite arms were approximately 30 and 50 μm, respectively. Heavy elements such as W and Mo with high melting points, tend to segregate at the core of the dendrites, leading to a lighter appearance, while the interdendrite region of the as-cast microstructure was enriched with Al and Ti [17]. Owing to segregation of the solute elements, the cast microstructure is expected to have different morphologies at different parts of the casting and to respond in different ways according to the γ' precipitate counts.

Fig. 2 shows the interdendritic γ/γ' colonies found at

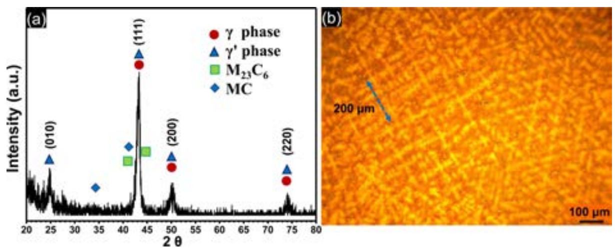

Fig. 1. (a) XRD pattern and (b) OM image of as-cast Rene 80 sample.

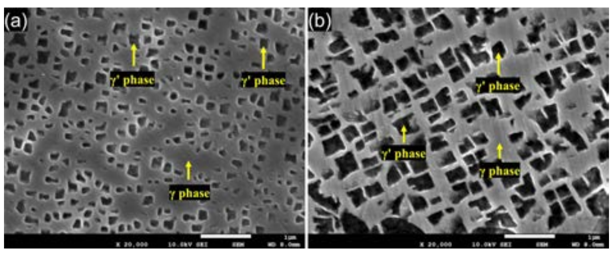

Fig. 2. FE-SEM images showing interdendritic γ/γ' colonies found at the interdendtritic zones. The microstructure has duplex size of (a) fine and (b) coarse γ' precipitates.

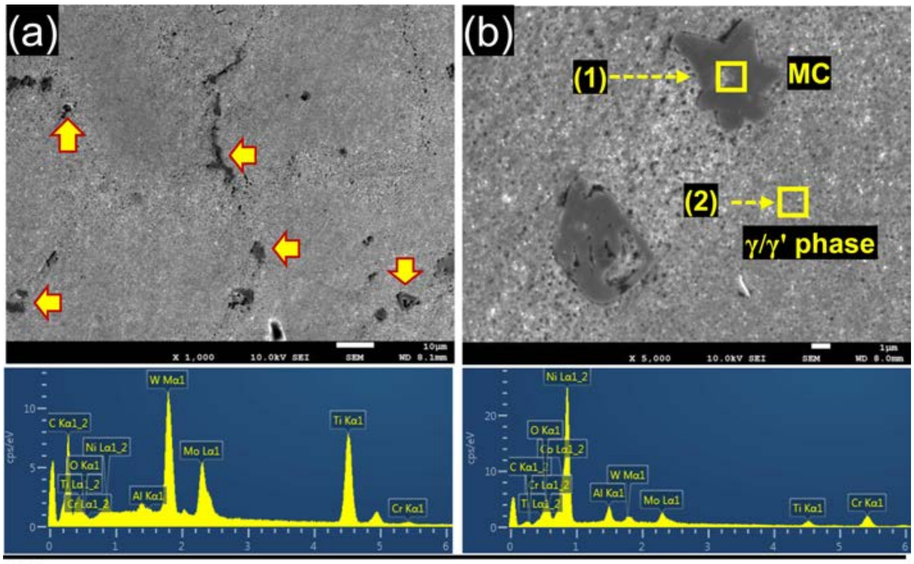

Elements (at.%)	C	Ni	Ti	Mo	W	Cr	Co	Al
(1)	50.96	2.16	32.95	6.00	5.98	1.27	0.46	0.23
(2)	5.25	48.71	4.38	3.21	0.97	17.62	9.71	5.14

Fig. 3. FE-SEM images and EDS results focused on the metal carbides. The precipitates are comprised of blocky and/or script metal carbides in the as-cast Rene 80 sample.

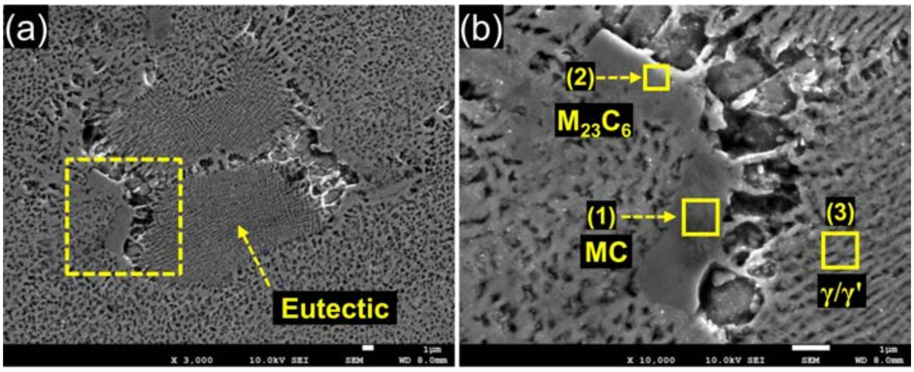

Elements (at.%)	C	Ni	Ti	Mo	W	Cr	Co	Al
(1)	50.25	1.35	29.66	8.06	2.95	2.21	0.46	0.52
(2)	12.83	13.26	4.36	25.88	3.90	34.06	-	0.85
(3)	9.34	43.50	3.25	2.88	0.95	18.64	9.57	4.66

Fig. 4. Morphology of the blocky MC and script $M_{23}C_6$ carbides and chemical compositions measured via EDS at grain boundaries.

the interdendtritic zones in the as-cast microstructure via FE-SEM. In the as-cast microstructure, bimodal precipitates of the γ' phase can be seen in Fig. 2. The bimodal γ' precipitates can be classified into spheroidal and cuboidal shapes in the nanoscale dimension. Fig. 2 shows that the microstructure has a duplex size with fine and coarse γ' precipitates. In the dendritic region, Fig. 2(a), there are fine γ' precipitates, while in the interdendritic region of Fig. 2(b), coarse γ' precipitates exist, also observed by Kim et al. [18]. The dendrite segregation of the alloy element plays an important role in the formation of the phase and solidification defect, such as the γ/γ' eutectic in the interdendritic area. This type of microsegregation negatively influences the mechanical properties of the superalloy and should be minimized as much as possible.

Fig. 3 shows FE-SEM micrographs of the metal carbides and the EDS analysis results. The as-cast Rene 80 Ni superalloy, with 0.17 wt.% carbon in this case, comprises blocky and/or script metal carbides in the as-cast structure shown in Fig. 3(a). The EDS examination revealed that these metal carbides with blocky and/or script morphologies and with average size of 5-10 µm, were MC carbides as shown in Fig. 3(b), where M denotes Ti, Mo, and W. The EDS results also show that the MC carbide is rich in Ti, Mo and W elements. These metal carbides were spread within the grains and on the grain boundaries. One of the characteristics of the distribution of these metal carbides is that they must spread consistently throughout the section, in such a way that there should not be more than 200 μm of distance between the metal carbides [19]. The regions depleted of metal carbides would be the soft areas that promote crack initiation in creep and fatigue at high temperatures.

The morphology shown in Fig. 4(a) indicates that the γ/γ' eutectic cell develops from sunflower to layer-built type because of the recrystallization of γ'. Fine γ' usually has a higher surface tension than the larger γ', and thus, it will more easily dissolve into the matrix. The growth of the γ' precipitate obeys the Lifshitz-Slyozov-Wagner law, which suggests a critical size and states that the particles with a size larger than the critical value would become coarse and those with a size smaller than the critical value would disappear [20]. Fig. 4(b) shows that the blocky MC and script $M_{23}C_6$ carbides are identified at the grain boundaries. The corresponding EDS indicates that the MC carbide is rich in Ti, Mo and W elements. The MC carbide is found at the grain boundaries or in the grain interior, which indicates that it is the most stable among the carbides and that Ti in Rene 80 can stabilize the MC carbide.

The presence of refractory metal elements such as W leads to the precipitation of the $M_{23}C_6$ carbide. After aging for a long time, metal carbides have enough time to provide carbon diffusion and react to form the $M_{23}C_6$ carbide. Choi et al. [21] found that the growth of $M_{23}C_6$ carbide at the grain boundary locally enriches the alloy with Al and Ti when the MC decomposes into $M_{23}C_6$, which enables to form the γ' particles along the grain boundary. The following reaction may lead to the formation of $M_{23}C_6$ carbide at the grain boundaries during heat treatment [22]:

$$MC + \gamma' \rightarrow M_{23}C_6 + \gamma'$$

Carbide-containing nickel-based superalloys have superior high-temperature mechanical properties compared with those strengthened only by the γ' phase. The presence of discrete carbides along the grain boundaries can prevent grain boundary sliding [23]. The $M_{23}C_6$ carbide that precipitates at the grain boundaries enveloped within layers of the γ' phase is the ideal morphology for inhibiting grain boundary sliding and improving creep resistance [24]. The precipitation of carbides prevents dislocation movement and grain boundary sliding, which can improve the mechanical properties of Rene 80.

Conclusions

The microstructure of the Ni-based superalloy Rene 80, prepared by investment casting, was investigated. The XRD results exhibited the prominent diffraction lines of the γ and γ' phases with MC and $M_{23}C_6$ metal carbides. OM images show that the microstructure of the as-cast Rene 80 consists of a two-phase γ/γ' microstructure with a dendrite segregation pattern. The carbides mainly consist of blocky MC and $M_{23}C_6$ in the as-cast Rene 80 sample. FE-SEM analyses showed that blocky MC and script $M_{23}C_6$ carbides were identified at the grain boundaries. The corresponding EDS results indicated that the MC carbide was rich in Ti, Mo, and W elements. The reaction $MC + \gamma' \rightarrow M_{23}C_6 + \gamma'$ led to the formation of the $M_{23}C_6$ carbide at the grain boundaries during heat treatment. The $M_{23}C_6$ carbide precipitated at the grain boundaries was enveloped within layers of the γ' phase, which is the ideal morphology for inhibiting grain boundary sliding and improving creep resistance.

Acknowledgments

This research was supported by Chunji Corporation and Nano Technology Laboratory of Korea National University of Transportation in 2017.

References

1. J. Tiley, G.B. Viswanathan, J.Y. Hwang, A. Shiveley, R. Banerjee, Mater. Sci. Eng. A 528 (2010) 32-36.
2. T. Goswami, Hänninen, Mater. Des. 22 (2001) 199-215.
3. T. Goswami, Hänninen, Mater. Des. 22 (2001) 217-236.
4. R.K. Sidhu, O.A. Ojo, M.C. Chaturvedi, J. Mater. Sci. 43 (2008) 3612-3617.
5. J.P. Collier, S.H. Wong, J.K. Tien, J.C. Phillips, Metall. Mater. Trans. A 19 (1988) 1657-1666.
6. Y. Xu, Q. Jin, X. Xiao, X. Cao, G. Jia, Y. Zhu, H. Yin, Mater. Sci. Eng. A 528 (2011) 4600-4607.
7. Y. Xu, C. Yang, X. Xiao, X. Cao, G. Jia, Z. Shen, Mater. Chem. Phys. 134 (2012) 706-715.
8. Y. Xu, C. Yang, X. Xiao, X. Cao, G. Jia, Z. Shen, Mater. Sci. Eng. A 530 (2011) 315-316.
9. M. Aghaie-Khafri, M. Hajjavady, Mater. Sci. Eng. A 487 (2008) 388-393.
10. F. Pyczak, S. Neumeier, M. Göken, Mater. Sci. Eng. A 510-511 (2009) 295-300.
11. C.N. Wei, H.Y. Bor, L. Chang, Mater. Sci. Eng. A 527 (2010) 3741-3747.
12. J. Safari, S. Nategh, J. Mater. Process. Technol. 176 (2006) 240-250.
13. W.R. Sun, J.H. Lee, S.M. Seo, S.J. Choe, Z.Q. Hu, Mater. Sci. Eng. A 271 (1999) 143-149.
14. C.N. Wei, H.Y. Bor, J. Alloys Compd. 509 (2011) 5708-5714.
15. C. Yang, Y. Xu, H. Nie, X. Xiao, G. Jia, Z. Shen, Mater. Des. 43 (2013) 66-73.
16. Z. Zhang, B.Q. Han, J.Y. Huang, Y.H. Han, Y. Zhou, K. Kakegawa, E.J. Lavernia, Metall. Mater. Trans. A 40A

(2009) 2023-2029.
17. G.E. Fuchs, Mater. Sci. Eng. A 300 (2001) 52-60.
18. M.T. Kim, S.Y. Chang, J.B. Won, Mater. Sci. Eng. A 441 (2006) 126-134.
19. H. Xuebing, K. Yan, Z. Huihua, Z. Yun, H. Zhuangqi, Mater. Lett. 36 (1998) 210-213.
20. I.M. Lifshitz, V.V. Slyozov, J. Phys. Chem. Solids 19 (1961) 35-60.
21. B.G. Choi, I.S. Kim, D.H. Kim, C.Y. Jo, Mater. Sci. Eng. A 478 (2008) 329-335.
22. T.J. Garosshen, G.P. Mccarthy, Metall. Trans. A 16 (1985) 1213-1223.
23. L.Z. He, Q. Zheng, X.F. Sun, G.C. Hou, H.R. Guan, Z.Q. Hu, J. Mater. Sci. 40 (2005) 2959-2964.
24. A.K. Jena, M.C. Chaturvedi, J. Mater. Sci. 19 (1984) 3132-3139.